

Manuscript prepared for SOOT FORMATION (Sarofim et al., eds.), Karlsruhe University Press, 2007,
follow-up on presentation by K. Kohse-Höinghaus, Anacapri Workshop, Italy, May 2007

Opportunities and issues in chemical analysis of premixed, fuel-rich low-pressure flames of hydrocarbon and oxygenate fuels using in situ mass spectrometry

K. Kohse-Höinghaus^{1*}, T. Kasper^{1,2}, P. Oßwald¹, U. Struckmeier¹,
N. Hansen², T. A. Cool³, J. Wang³, F. Qi⁴, P. R. Westmoreland⁵

¹*Department of Chemistry, Bielefeld University, Universitätsstraße 25, D-33615 Bielefeld,
Germany;*

²*Combustion Research Facility, Sandia National Laboratories, Livermore, CA 94551, USA;*

³*School of Applied and Engineering Physics, Cornell University, Ithaca, NY 14853, USA;*

⁴*National Synchrotron Radiation Laboratory, University of Science and Technology of China,
Hefei, Anhui 230029, P. R. China;*

⁵*Department of Chemical Engineering, University of Massachusetts, Amherst, MA 01003,
USA*

*corresponding author

Katharina Kohse-Höinghaus

Department of Chemistry

Bielefeld University

Universitätsstraße 25

D-33615 Bielefeld

Germany

Email: kkh@pc1.uni-bielefeld.de

Phone : +49 521 106 2052

Fax : +49 521 106 6027

KEYWORDS. fuel-rich flames, molecular beam mass spectrometry, intermediate species
concentrations, combustion chemistry, biofuels

Opportunities and issues in chemical analysis of premixed, fuel-rich low-pressure flames of hydrocarbon and oxygenate fuels using *in situ* mass spectrometry

**K. Kohse-Höinghaus^{1*}, T. Kasper^{1,2}, P. Oßwald¹, U. Struckmeier¹,
N. Hansen², T. A. Cool³, J. Wang³, F. Qi⁴, P. R. Westmoreland⁵**

¹*Department of Chemistry, Bielefeld University, Universitätsstraße 25, D-33615 Bielefeld, Germany;*

²*Combustion Research Facility, Sandia National Laboratories, Livermore, CA 94551, USA;*

³*School of Applied and Engineering Physics, Cornell University, Ithaca, NY 14853, USA;*

⁴*National Synchrotron Radiation Laboratory, University of Science and Technology of China, Hefei, Anhui 230029, P. R. China;*

⁵*Department of Chemical Engineering, University of Massachusetts, Amherst, MA 01003, USA*

Abstract

A rich pool of minor species, including radicals, is assumed to be important for the detailed chemical reaction network in the molecular phase which precedes the formation of polycyclic aromatic hydrocarbons (PAH) and soot. For a realistic simulation of fuel-rich chemistry in hydrocarbon- and oxygenate-fuelled flames, the development and validation of respective models requires interaction with reliable experiments. One useful environment to study fuel-rich chemistry is a premixed low-pressure flame, where major and intermediate species concentrations can be obtained experimentally with good spatial resolution. Here, we focus on molecular beam mass spectrometric (MBMS) techniques, which are applied *in situ* to measure the chemical composition in low-pressure flames of different neat fuels and fuel blends, including hydrocarbons, alcohols, ethers and esters. Three different ionization techniques are employed, including resonance-enhanced multi-photon ionization (REMPI), electron ionization (EI), and vacuum ultraviolet photoionization (VUV-PI) using tunable synchrotron radiation. We concentrate here on several aspects of these studies. A large part of this article is devoted to a discussion of quantitative measurements and typical error limits, especially regarding intermediate species. Further, we focus on concentration measurements of intermedi-

ates which are assumed to be involved in the formation of the first and second ring from aliphatic fuels. Strategies are now available to provide isomer-specific information from the study of flames burning hydrocarbon and oxygenate fuels and mixtures thereof – information which is only partially reflected in present flame models.

1. Introduction

Because of their perceived potential to reduce undesired combustion emissions, biofuels are discussed as one alternative to conventional hydrocarbon fuels of fossil origin [1]. Fuels obtained from biological sources, e.g. plant matter or organic waste, are thought to have a beneficial impact on the emission of carbon dioxide from combustion devices. They are also being used or discussed as oxygenated additives of neat fuels, since they may decrease the emission of particulate matter. To assess their emission potential, however, either as a neat fuel or as fuel additive, more detailed investigation of their combustion chemistry is highly desirable. A huge body of information on hydrocarbon combustion chemistry is available, including the results of decades of collaborative work of experimental and modelling groups. They have studied aliphatic and aromatic hydrocarbon fuel decomposition and oxidation and investigated the mechanism of soot formation in shock tubes, flow reactors, flames, rapid compression machines and other reactive combustion environments; important aspects of hydrocarbon combustion can now be reliably modelled and predicted. In contrast, similarly detailed studies of oxygenated fuels are comparatively rare. Many features in oxygenated fuel combustion chemistry should, of course, be quite similar - small hydrocarbon radicals will be formed in the decomposition process, and the build-up of larger hydrocarbon molecules including aromatic structures, polycyclic aromatic hydrocarbons (PAH) and soot may potentially proceed from the same hydrocarbon intermediates. The pool of active intermediate species will depend to a certain extent on the fuel structure, however, and the additional functional groups in the oxygen-containing fuel molecule will give rise to new sets of intermediates and reaction products that may not be formed or not be of similar importance in hydrocarbon combustion. In particular, the formation of aldehydes, including formaldehyde and acetaldehyde, needs further study since these are hazardous air pollutants.

In recent years, our groups have contributed to the investigation of several aspects of fuel-rich flame chemistry in hydrocarbon and oxygenate fuel flames and fuel blends as part of an ongoing collaboration. Detailed studies have been performed to measure quantitative concentrations of families of flame species, including main constituents as well as stable and radical

intermediates. To facilitate comparison with chemical-kinetic modelling, premixed, one-dimensional flames have been studied, mostly at low pressures around 50 mbar. The emphasis in our experiments has been on the molecular phase preceding soot; thus, stoichiometries have been selected which permit formation of small aromatic compounds from aliphatic fuels, but do not produce soot. Flames of oxygenated fuels have been studied using similar stoichiometries. Since the development and optimization of chemical reaction mechanisms will depend on reliable experimental information, the emphasis is to determine quantitative species concentration profiles. The experimental strategies will thus be discussed in light of potential sources for measurement errors. The discussion will concentrate on the chemistry in the molecular phase that precedes PAH and soot formation with an additional focus on the role of isomer-specific information.

2. Quantitative species concentration profiles

Quantitative measurements of intermediate species in flames have a long tradition, with laser spectroscopy as one of the major instruments for the detection of small radicals. Laser-induced fluorescence (LIF), cavity ringdown spectroscopy (CRDS), degenerate four-wave mixing (DFWM) and other sensitive laser spectroscopic techniques and their specific advantages and applications have been discussed in textbooks and reviews [2-5]. Under low-pressure premixed fuel-rich flame conditions, these non-invasive spectroscopic techniques are very useful to measure the flame temperature and concentrations of some smaller radicals. As a more generally suited technique, molecular beam mass spectrometry (MBMS) has been developed [6-12], which probes the flame by means of an invasive sampling nozzle. The gas sample is introduced into a mass spectrometer with special care to quench further reaction and avoid fragmentation. Several strategies for ionization have been used in this work, including electron ionization (EI), resonance-enhanced multi-photon ionization (REMPI) and vacuum ultraviolet photoionization (VUV-PI).

Coupling laser diagnostics and mass spectrometry permits an extensive species pool analysis. In fuel-rich, non-sooting low-pressure flames, such strategies have been used to investigate the molecular precursor phase of larger PAH and soot [13,14]. The flame front under these conditions is especially rich in hydrocarbon radicals which may be involved in the build-up of higher molecular structures. The detection of a certain species, however, does not provide information about its importance in the process. The species profiles are thus typically compared with full simulations of the entire reaction network up to benzene and beyond. Many

details about the formation of the first aromatic ring in flames have been obtained using this approach.

2.1 Temperature

If a model is to be developed, extended and validated on the basis of measured species profiles, the measurements are expected to provide optimum reliability. For such a comparison of experiment and model, the analysis typically includes measurement of an accurate temperature profile (from fresh to burnt gases): the temperature rise throughout the flame zone is particularly important, and flames stabilized on water-cooled disk-shaped burners as in this study will not attain fully the temperature calculated from adiabatic equilibrium. If a series of stoichiometries for the same fuel is studied without changing the mass flow, the stand-off distance of the flame front to the burner may be different, leading to different cooling effects; e.g. the flame front in a stoichiometric flame is closer to the burner surface than in a fuel-rich flame and is therefore subjected to larger cooling by the burner. Temperature measurement strategies and their implications have been discussed in the literature [2,15,16]. In the fuel-rich, premixed, laminar low-pressure flames discussed here, the temperature profile has mostly been obtained by LIF of OH or of seeded molecules such as NO following the approach described in [17] or, more sensitively, by CRDS of OH as detailed in [18]. The typical error is ≤ 80 K at a flame temperature of ≥ 2000 K. Especially high precision can be obtained in NO-LIF temperature measurements with fits to multiple spectral lines, using extended spectroscopic databases and appropriate fitting routines [19]; here, the procedure by Atakan et al. was adopted [19b]. In combination with species profiles from MBMS measurements, however, it may be problematic that a non-invasive optical temperature measurement is usually performed without the presence of a sampling nozzle [20,21]. To compare with modelling, it must thus be determined whether a shift of the measured species profiles will account quantitatively for such probe effects, a procedure which may be questioned [21]. Temperature is often also measured by thermocouples, where care must be taken to avoid catalytic effects and to correct for radiative and other heat losses. Recently, it has been demonstrated that thermocouples coated with a thin alumina layer by chemical vapor deposition (CVD) can provide results in close agreement with optical methods in some of the flames studied here [22].

2.2 Species profiles

Similar care is required for the quantification of species concentrations, and protocols to achieve accurate data have been developed, often independently, in many laboratories. For

LIF measurements, the data evaluation needs accurate, quantitative fluorescence quantum yields, and for CRDS and other absorption techniques, the respective absorption coefficient must be known quantitatively. The mass spectrometric measurement can rely on calibration gases for stable molecules, but such procedures are not feasible for radicals. The absolute calibration will need a cross section for the specific ionization process (i.e. for electrons or photons), and it must accommodate insufficient mass resolution/partial overlap, fragmentation, auto-ionization resonances, and other potentially problematic influences. Also, mass discrimination factors (due to different radial velocities of the species) and a temperature-dependent sampling function (considering changing gas density) may have to be taken into account. Often, it may be helpful to calibrate a radical with respect to a related stable species, using procedures given in the literature [6-12]. Despite all efforts devoted to calibration issues, results of different techniques may be in “excellent” agreement if they deviate by only 20-30%, and “quite good” agreement may still be claimed if the results agree within a factor of 3. This seems reasonable for the combined error regarding radicals that are quantified using estimated cross sections for both electron ionization and VUV photoionization. Uncertainties of this order should be kept in mind when comparing measured, potentially “shifted” profiles to simulation/modelling results with the aim to verify chemical-kinetic model assumptions.

2.3 “Standard” flame conditions and typical uncertainties

We have adopted several precautions in our strategy to provide quantitative results on fuel-rich combustion chemistry. One useful approach is to define “standard” flame conditions which are repeatedly re-investigated whenever changes in the experimental apparatus or procedures are performed, or when nominally identical flame conditions are studied in different set-ups or laboratories. A fuel-rich low-pressure propene-oxygen-argon flame with a C/O ratio of 0.77 [23] has been used for this purpose in our laboratory, and the resulting intermediate species concentrations have typically shown agreement of a factor of two or better. To investigate more than one stoichiometry for the same fuel extends the basis for a potential model comparison. As an example in a propene-oxygen-argon (25%) flame at 40 mbar with a C/O ratio of 0.5, Fig. 1 presents a quantitative comparison of several species mole fraction profiles resulting from VUV-PI measurements at two different measurement cycles. Identical equipment was used in both measurement periods, and data acquisition and evaluation procedures were kept unchanged.

Figure 1 presents three important species which are involved in the build-up of hydrocarbon structures: acetylene (C_2H_2), propargyl radical (C_3H_3), and benzene (C_6H_6); all can be calibrated using known ionization cross sections, fulvene concentration was below the detection limit. It is noted that acetylene persists beyond the flame front with a non-zero concentration in the burnt gas up to about 8-9 mm, and it may be involved in the reactions toward larger hydrocarbon structures in this broad range, while propargyl and benzene are exclusively found in the flame front with a maximum near 3.5 mm and negligible mole fractions above 5 mm. The shape of both sets of curves in Fig. 1 agrees quite well, but there are differences on the absolute scale which need further explanation. The differences for acetylene are within less than 10%, for benzene, the agreement is within about 30%, and the agreement for propargyl is within about 50%. The error bars for the measurement are indicated, and in each case, the results agree considering combined errors. Several features in Fig. 1 should be noted to appreciate this result. First, acetylene is present in the highest concentrations (in the percent level) of the three species, while maximum benzene mole fractions are a few tens of ppm in this not overly rich flame, which is close to the typical detection limit. Propargyl radicals attain maximum mole fractions of about 100 ppm. Thus, signal-to-noise ratio is different and plays a significant role. The ionization energy must be chosen as a compromise regarding different ionization potentials, achievable signal strength and potential fragmentation.

Second, it is interesting to consider the nominal error in the experimental conditions and calibration procedures. Typical errors in the stoichiometry (flow controller settings with up to 5% stated accuracy per individual gas flow, if gas correction factors are used) may amount to about 10%, photodiode calibration was estimated with 5% error, mass discrimination factors were determined from the two different runs with 15% uncertainty, temperature-dependent sampling functions which reflect the changing gas density are within about 15% uncertainty, and ionization cross sections are assumed to be known within 20%. An error analysis for repeated, careful measurements with the same apparatus reveals that 30% deviation for “well-behaved” species is not unexpected. Errors may be larger for smaller signal-to-noise ratios (lower species concentrations or lower cross sections), or when fragmentation or poorer mass resolution have to be taken into account. The almost perfect agreement in the case of acetylene in Fig. 1 may thus seem somewhat fortuitous and is linked to the fact that C_2H_2 concentrations do not change dramatically with the flame parameters. Also, if a cross section must be estimated, or if isomers cannot be fully resolved, the measurements will exhibit accordingly larger error limits.

2.4 Comparison of different MBMS techniques, role of mass and energy resolution

Knowledge of experimental accuracy, as demonstrated above for repeated measurements using a single set-up, can provide important guidance when comparing model calculations with experimental profiles, especially if kinetic parameters such as rate coefficients and their temperature dependences are varied to match the measured concentrations. It is similarly instructive to compare results for the same species under nominally identical flame conditions with different MBMS techniques. Such comparisons have been reported in [24], for example, where benzene concentrations in a C/O 0.77 propene-oxygen-argon flame are seen to agree within about 30% between EI-MBMS and VUV-PI-MBMS; the mole fraction has recently been confirmed also by REMPI-MBMS [25]. The different techniques and instruments exhibit complementary advantages and drawbacks, especially regarding energy and mass resolution. In the EI experiments, the mass resolution is $m/\Delta m \approx 3000$, enabled by a time-of-flight (TOF) instrument with reflectron, while it is ≈ 400 -600 for the linear instrument using VUV-PI. The energy distribution in the former experiment is quite broad, enabling detection of all species including Ar at a nominal ionization energy of 10.5 eV, while the energy resolution is $\Delta E (fwhm) \approx 40$ meV in the latter. The requirements for unambiguous species identification and quantitative interpretation of the mass spectra are even more acute when studying oxygenate flames, since numerous oxygenated intermediates will lead to additional features and potential overlaps.

The effect of mass resolution is illustrated in Fig. 2 where a spectrum near a mass-to-charge ratio m/z of 44 is displayed for EI (top row) and VUV-PI (bottom row) measurements [26]. The two-dimensional images on the left provide the signal intensity (for an increment of 0.25 amu) as a function of height above the burner (HAB). The EI data show the three individual peaks of CO_2 , $\text{C}_2\text{H}_4\text{O}$ and C_3H_8 at $m/z = 43.98$, 44.03 and 44.06, respectively. These features are clearly resolved as shown in the mass spectra at heights of 0.5 and 1.8 mm. The signatures exhibit a Gaussian shape, and individual peak intensities can be determined from a fitting routine. The same signatures overlap and appear as a single broad peak in the VUV-PI experiment, but can be distinguished by their ionization energies. In addition, contributions of both acetaldehyde and ethenol to $\text{C}_2\text{H}_4\text{O}$ can be separated using VUV-PI [27]. At 25 mm above the burner, the contribution of CO_2 is dominant. Note also that the signals are much smaller in the EI-MBMS measurement.

Especially when species with weaker bond strengths are to be detected in the EI-MBMS experiment, fragmentation may occur already at nominal ionization energies near the ionization potential. The rather broad energy distribution does not permit to separate fragmentation products easily from the flame species with the same chemical composition. This is illustrated in Fig. 3 for a cold gas sample of ethanol. All traces are normalized to the signal intensity of the parent ion (mass 46) at 12 eV. In the EI measurements it is obvious that signals from fragmentation products at $m/z=31$ (CH_3O) and 45 ($\text{C}_2\text{H}_5\text{O}$) produce higher signal intensities than the parent ion itself. Furthermore, strong signals of the parent and fragment ions can already be detected below the ionization potential of ethanol of 10.48 eV [28], which can be ascribed to the presence of electrons with a higher than the nominal ionization energy. In the PI experiment, ethanol ions can be produced separately from its fragment ions – which appear at higher ionization energy – as shown in the right panel of Fig. 3.

A more detailed comparison of species profiles in a fuel-rich ethanol flame, measured with both EI-MBMS (symbols) and VUV-PI-MBMS (solid lines), is presented in Fig. 4. Here, the results for major species, acetylene, ethylene, formaldehyde and the propargyl radical are given; profiles from the photoionization measurements have been shifted by 0.4 mm to larger distances from the burner to match the peak positions [26]. A shift of this order may have several reasons, including uncertainties in the stoichiometry, in determining the zero height position, different sampling orifice diameters and different cooling effects of the burner and the sampling probe. Temperature profiles in both configurations are indicated; they have been obtained without the presence of a sampling cone. Differences at smaller heights are attributed to different heat transfer to the burner in the two instruments. In general, the agreement between both sets of measurements is quite good. Major species mole fraction profiles agree well in the burnt gases, with the exception of H_2 and H_2O , and deviate somewhat earlier in the flame, especially for O_2 and fuel. The latter effect may be related to different heat transfer and diffusion. The discrepancy between H_2 and H_2O profiles has been noted before in these experiments; this suggests the influence of an instrumental parameter such as the accumulation of background gases [26]. The peak mole fractions of the stable intermediate products (C_2H_2 , C_2H_4 , CH_2O) agree within 10-15%, and peak position and shape of the profiles are also in very reasonable agreement.

We thus conclude, in particular with respect to the rich pool of intermediates encountered in fuel-rich hydrocarbon- and oxygenate-fuelled flames, that species profiles of stable and radi-

cal intermediates can be provided with high confidence levels when experiments with high energy and mass resolution are combined, and when calibration samples and/or absolute cross sections for the ionization process in question are available. This does not resolve the issue of sampling probe effects; for this, comparison with optical measurements is highly desirable.

3. Formation of benzene and further small aromatics

In the study of fuel-rich flames, we have mainly concentrated on the detection of species involved in the formation of the first aromatic ring as a function of the fuel structure. Flames of several C₂-, C₃- and C₅-fuels were studied in particular, including acetylene [29], propene [23,29], cyclopentene [30], 1-pentene [31], 1,3-pentadiene [32] and fuel blends [32]. Pressure and C/O ratio, C/H ratio or both were kept fixed when the fuel was changed in the same experimental environment. Temperature was typically measured with LIF, and species concentrations of the major species and many intermediates of the C_xH_y type with 1≤x≤6 and 1≤y≤10 were obtained from EI-MBMS [29,33] using direct calibration or cross section estimation procedures from the literature [6]. The results provided strong indications for fuel-dependent importance of the different pathways yielding benzene [32]. In a comparison of flames of propene and of several C₅-fuels, C₃H₃ recombination was seen to be of importance in all flames studied, while contributions of other reactions depended on the specific decomposition pattern of the fuel and the corresponding intermediate pool [32]. It should be noted that the perceived relative importance of a specific reaction will depend on its temperature-dependent rate coefficient. Some of the key reactions continue to be investigated, hopefully eliminating remaining uncertainties in their rate coefficients, so that the relative importance of a specific pathway for a given flame condition may be ascertained [25,32]. Some of the results from these earlier studies have been modelled [34-38] with quite good agreement. Well-predicted features include the benzene concentration and some key intermediates like propargyl.

3.1 Mole fraction ratios for small aromatic species beyond benzene

While the EI-MBMS method is well suited to provide an overview of the species pool, its sensitivity for larger aromatic species beyond benzene is limited. Here, REMPI-MBMS has been used to identify aromatic intermediates up to $m/z \approx 200$ in fuel-rich propene and cyclopentene flames [25]. Since both flames have been investigated with the same instrument under identical conditions, it has been assumed that the ratios of the respective REMPI signals at a given m/z will reflect the concentration ratio of this species. The reliability of the REMPI

method has been demonstrated for the example of benzene, where independent, quantitative MBMS measurements with EI and REMPI (and, most recently, VUV-PI-MBMS) resulted repeatedly in good agreement [24,25,39]. For several aromatic intermediates, including benzene, toluene, phenol, phenylacetylene, styrene, naphthalene and others, the **ratios** of their REMPI signals in both flames (i.e. of the respective species mole fractions) were thus determined: they are of the order of 3-10, with the cyclopentene flame generally providing higher concentration levels. These ratios have been measured in flames of both fuels with identical stoichiometry (C/O ratio), initial gas flow and pressure, and have been corroborated using VUV-PI-MBMS [40]. Such relative measurements can be particularly useful since the influences of insufficiently well known parameters will cancel. This was also a preferred approach in modelling the two flames, in addition to comparing selected individual profiles [25]. Effects of poorly known kinetic data might in fact cancel in some cases, and predicted concentration **ratios** could still be reliable. If pathways are very different in the two flames, however, this might be revealed from the comparison of predicted and measured ratios, and key reaction sequences can be analyzed via reaction flow and sensitivity analysis.

In our investigation [25], many features of the reaction network leading to benzene were predicted quite reasonably, while intriguing differences of up to several orders of magnitude were observed between the measured and simulated mole fraction ratios for small aromatic compounds beyond benzene. Overprediction of the mole fraction ratio can occur when the respective species concentration is overestimated in the cyclopentene flame, or if it is underestimated in the propene flame, or both. The modelling attempt [25] has not revealed an easy explanation of the observed behavior, and many details deserve further study. It is highly plausible, however, that the particularly rich chemistry of the cyclopentene flame, which involves some reactions sequences for which the kinetics are still under debate, may need further investigation. Most recently, an independent data set for the same cyclopentene flame has been provided [38] using VUV-PI-MBMS, with many intermediate species in good agreement with the earlier measurements [30].

3.2 Oxygenated additives, trends in benzene and aromatics formation

Aromatics formation as well as soot emission is assumed to be reduced in flames of oxygenated fuels or flames doped with oxygenates. Thus, flame chemistries have been studied using the same combinations of methods, for example, for ethanol [39], dimethyl ether [41] and other oxygenated fuels. This demands identification of additional oxygenated intermediates

not present in pure hydrocarbon flames. Experimental challenges include an increasing tendency of fragmentation of species with labile bonds and more overlaps of peaks in the mass spectra. Families of flames with different amounts of oxygenated additives were studied [24], with substantial increase in the number of profiles to be recorded, evaluated and, eventually, compared to models. As expected, preliminary analysis of the combustion chemistry of oxygenates and of hydrocarbon-oxygenate mixtures shows a tendency to decrease the concentrations of aromatic species, at the expense of an increase of some oxygenated compounds, however, including aldehydes [24,39].

As an example, Fig. 5 shows the maximum signal intensities of aromatic molecules in ethanol-blended propene flames ($C/O=0.6$) with varying ethanol fraction from 0-60% in the fuel mixture, normalized to those in the unblended propene flame. An almost linear decrease is evident for most detected compounds, including benzene at $m/z = 78$, toluene at $m/z = 92$, phenol at $m/z = 94$, indene at $m/z = 116$ and naphthalene at $m/z = 128$ [39]. An even more pronounced decrease was observed for a propene-ethanol-oxygen-argon flame series at $C/O=0.773$ [39], where the ethanol fraction in the fuel could be varied from 0-15%. The complete replacement of propene by ethanol was recently studied in a series at $C/O=0.5$ [24,42], and a similar analysis was performed for hydrocarbon and oxygenated intermediates.

Figure 6 shows trends in the maximum mole fractions for selected hydrocarbon species in these ethanol-blended propene flames with changing ethanol fraction in the fuel mixture. The effect of changing fuel composition is shown in a ratio γ , depicted on the ordinate, which is defined as maximum mole fraction of the individual species in the blended flame normalized by that in the pure propene flame. The behavior of many hydrocarbon intermediates is seen to fall into two categories, which are illustrated by the shaded areas in Fig. 6: those which show a pronounced decrease of more than a factor of 3, and those which show a less substantial decrease of about a factor of 2 or less. In the first category, C_3 intermediates common to the propene flame are found such as C_3H_3 , allene, propyne and C_3H_5 , together with vinyl acetylene and benzene itself. Methyl, ethylene and acetylene show a less pronounced effect. Many of these small intermediates are involved in aromatic hydrocarbon growth, and details of the influence of ethanol on this chemistry are under study. Trends in the maximum mole fractions of some oxygenated intermediates are shown in Fig. 7 for the same set of flames. The ratios given here have been normalized to the pure ethanol flame, to avoid division by a small number, since the acetaldehyde and ethenol concentrations in the pure propene flame are rather

low. A preliminary analysis shows that the formaldehyde mole fraction changes by about a factor of two or less, while both acetaldehyde and ethanol are lower in the pure propene flame by about an order of magnitude.

A quantitative analysis of the impact of these findings with regard to emission regulations must consider, however, that temperature and composition will be changed by replacement of one fuel with the other. Effects of the **interaction** of hydrocarbon and oxygenate chemistries [41,42] will be resolved only by analyzing the species pool in accurate, quantitative detail and by eventually modelling the specific conditions.

4. Isomer-selective chemistry

Since the availability of tunable synchrotron radiation with high photon flux and energy resolution, the chemistry of fuel-rich flames can be studied in unprecedented detail, with the main advantage that isomeric species can be unambiguously identified. While REMPI-MBMS can specifically detect isomers whenever suitable radiative transitions are known, synchrotron-based flame mass spectrometers can employ energy-selective detection more generally [43,44]. Typically, a flame study can now be performed routinely with respect to several dimensions in an “imaging” analysis [45]. Flame species are detected according to their mass in the range up to about $m/z \approx 200$ either in “burner scans” at a given energy, where the distance from the burner is varied to provide species profiles, and they can also be recorded at a given distance from the burner in “energy scans”, where different ionization thresholds permit identification of several isomers at a given mass when the ionization energy is scanned. Two-dimensional color-coded intensity matrices of photon energy or height above the burner versus mass-to-charge ratio, as seen in Fig. 2, may be viewed as representation of key features of the combustion chemistry at a given flame condition.

4.1 Identification of “new” species

The technique has been instrumental in the identification of species never detected in a flame before, such as enols [27], an example for which was also shown in Fig. 7. Another example is the quantitative measurement of the two isomers of C_3H_4 , allene and propyne [24,43], which are involved in different pathways in aromatics formation [46]. With respect to the cyclopentene flame mentioned above, the analysis using this method has tentatively identified at least two cyclic species of chemical composition C_7H_6 ($m/z=90$) and two or more cyclic species of formula C_7H_8 ($m/z=92$) [38]. Some of them are not included in present mechanisms

for aromatics and soot formation, and their role in this process – if any – is yet unknown. Further details in the analysis of many flames using this method may reveal “new” species, the combustion reactions of which (and their respective kinetic, thermodynamic and transport data) will not – or not precisely – be known under such conditions. While the “discovery” of such new species may be a satisfactory result in itself, it may eventually slow down the process of flame model development, because some information may turn out to be unimportant after all.

4.2 Study of isomeric fuels

Another approach in isomer-selective flame chemistry makes use of the advanced measurement capabilities of synchrotron flame instruments in the investigation of isomeric fuel combustion under identical conditions. The two isomers of propanol have been studied [47] and the respective species mix is found to be quite different, in particular with respect to aldehyde formation. The four butanol isomers [48,49] show a distinctly different species pool in all four flames – not unexpectedly regarding the fuel decomposition reactions to different radical species. Similarly, the combustion of isomeric esters [50,51] is being investigated. Again, the results show the importance of fuel-specific decomposition pathways which result in different concentrations of intermediates, although temperature and main species concentration profiles are almost indistinguishable.

As an example, results from flames of the four isomers of butanol are shown in Figs. 8 and 9 [48] to illustrate the potential of the technique. Figure 8 shows the isomers of mass 72 determined in the four flames. Butanal is detected in the 1-butanol flame, 2-methyl-propanal in the *iso*-butanol flame, 2-butanone in both the 2-butanol and *tert*-butanol flames, indicating that the carbonyl function is detected at the position of the OH group in the fuel, except in the *tert*-butanol flame, where formation of 2-butanone is possible upon C-C bond fission. Also, butenols are seen to be present. Similarly, differences are seen with respect to further decomposition products from the fuel, for example at $m/z = 58$ (C_3H_6O), where acetone is seen in the *tert*- and 2-butanol flames and propanal in the *iso*- and *tert*-butanol flames. Also, for $m/z = 56$ ($C_4H_8 + C_3H_4O$), 1-butene is formed in the *tert*- and 1-butanol flames, 2-butene in the 2-butanol flame, and further species including methylketene and 2-methylpropene are also identified. The decomposition products generally show good agreement with the expected breakdown of the molecules, with a noticeable dependence of oxygenated intermediates on fuel structure, and a less pronounced dependence of the hydrocarbon intermediates on fuel struc-

ture. As shown in Fig. 9, the build-up of benzene as the first aromatic ring is seen in all four flames, with fulvene also being detected as a further C₆H₆ isomer.

The exploration of isomer-selective combustion chemistry in this level of detail has only recently begun, and opportunities to resolve previously unobserved details in combustion chemistry are expanding. The wealth of experimental results, of which only a few examples could be illustrated here, and which could only be achieved through close multi-national collaboration, must now be considered as an important source of information in the development of hydrocarbon and oxygenate combustion models.

5. Conclusions

Detailed analysis of fuel-rich flame chemistry was discussed focussing on combinations of different mass spectrometric techniques. Examples were demonstrated from laminar, premixed low-pressure flames, using molecular beam mass spectrometry with electron ionization, resonance-enhanced multi-photon ionization, and photoionization with tunable vacuum UV radiation from synchrotron sources. Some attention was given to the discussion of typical uncertainty levels for stable and radical species, and to the comparison of the results obtained with a combination of techniques in several laboratories. The attainable accuracy depends largely on the availability of absolute ionization cross sections of the species in question and/or of sample gases of known concentrations; also, energy and mass resolution as well as fragmentation problems must be considered. The MBMS instruments were used to study fuel-rich hydrocarbon combustion in propene and cyclopentene flames, and have revealed remarkably large differences between predicted and measured concentration ratios for some aromatic species beyond benzene. The understanding of how the second and third aromatic rings are formed in premixed flames of aliphatic fuels from molecular precursors needs further investigation. Also, the effect of oxygenated additives such as ethanol has been studied in families of propene flames. As a first tendency, benzene and its precursors are seen to decrease in concentration, while some oxygenated species are formed in larger concentrations when propene is replaced by ethanol. Quantification and interpretation of these effects will be forthcoming and will eventually need modelling to resolve the influence of temperature on the observed changes. As a major breakthrough in mass spectrometric analysis of combustion chemistry, the potential of isomer-selective detection and of the study of isomeric fuels has been demonstrated. Clearly, “new” species which had not been detected with conventional instruments must be investigated further with respect to their roles. Also, the discussion of

bio-derived fuels with respect to cleaner and potentially CO₂-efficient or CO₂-neutral combustion may encourage study of flames with fuels that exhibit even further functional groups. It may be a challenge to select the experiments which will provide reliable, quantitative and useful data for advancing soot models regarding such fuels and fuel-blends, and which will address remaining open questions in fuel-rich hydrocarbon combustion.

References

1. Basic Research Needs for Clean and Efficient Combustion of 21st Century Transportation Fuels, Office of Science, US Department of Energy, BES Workshop November 2006, available also at www.sc.doe.gov/bes/reports/list.html
2. A. C. Eckbreth, *Laser Diagnostics for Combustion Temperature and Species*, Second edition. Gordon and Breach, UK, 1996.
3. K. Kohse-Höinghaus, *Prog. Energy Combust. Sci.* 20 (1994) 203-279.
4. K. Kohse-Höinghaus, R. S. Barlow, M. Aldén, J. Wolfrum, *Proc. Combust. Inst.* 30 (2005) 89-123.
5. K. Kohse-Höinghaus, J. B. Jeffries (Eds.), *Applied Combustion Diagnostics*. Taylor and Francis, New York, 2002.
6. J. C. Biordi, C. P. Lazzara, J. F. Papp, *Prog. Energy Combust. Sci.* 3 (1977) 151-173.
7. K. Bonne, K. H. Homann, H. Gg. Wagner, *Proc. Combust. Inst.* 10 (1965) 503-512.
8. J. Peeters, G. Mahnen, *Proc. Combust. Inst.* 14 (1973) 133-146.
9. A. Bhargava, P. R. Westmoreland, *Combust. Flame* 115 (1998) 456-467.
10. J. Vandooren, M. C. Branch, P. J. van Tiggelen, *Combust. Flame* 90 (3-4) (1992) 247-258.
11. K. H. Homann, *Angew. Chem. Int. Ed.* 37 (18) (1998) 2434-2451.
12. J. H. Werner, T. A. Cool, *Combust. Flame* 117 (1998) 78-98.
13. H. Bockhorn (Ed.), *Soot Formation in Combustion*, Springer-Verlag, Berlin, 1994.
14. C. S. McEnally, L. D. Pfefferle, B. Atakan, K. Kohse-Höinghaus, *Prog. Energy Combust. Sci.* 32 (3) (2006) 247-294.
15. W. P. Stricker, in: K. Kohse-Höinghaus, J. B. Jeffries (Eds.), *Applied Combustion Diagnostics*. Taylor and Francis, New York, 2002, 155-193.
16. N. M. Laurendeau, *Prog. Energy Combust. Sci.* 14 (1988) 147-170.
17. A. T. Hartlieb, B. Atakan, K. Kohse-Höinghaus, *Appl. Phys. B* 70 (2000) 435-445.
18. a) K. Kohse-Höinghaus, A. Schocker, T. Kasper, M. Kamphus, A. Brockhinke, *Z. Phys. Chem.* 219 (2005) 583-599, and b) A. Schocker, K. Kohse-Höinghaus, A. Brockhinke, *Appl. Optics* 44 (31) (2005) 6660-6672.
19. a) W. G. Bessler, C. Schulz, V. Sick, J. W. Daily, *A versatile modeling tool for nitric oxide LIF spectra*, Proceedings of the Third Joint Meeting of the U.S. Sections of The Combustion Institute (Chicago, March 16-19, 2003, paper PI05), <http://www.lifsim.com>. and b) B. Atakan, J. Heinze, U. E. Meier, *Appl. Phys. B* 64 (1997) 585-591.

20. P. Desgroux, L. Gasnot, J. F. Pauwels, L. R. Sochet, *Combust. Sci. Technol.* 100 (1994) 379-384.

21. A. T. Hartlieb, B. Atakan, K. Kohse-Höinghaus, *Combust. Flame* 121 (2000) 610-624.

22. N. Bahlawane, U. Struckmeier, T. S. Kasper, P. Oßwald, *Rev. Sci. Instrum.* 78 (2007) 013905.

23. B. Atakan, A.T. Hartlieb, J. Brand, K. Kohse-Höinghaus, *Proc. Combust. Inst.* 27 (1998) 435-444.

24. K. Kohse-Höinghaus, P. Oßwald, U. Struckmeier, T. Kasper, N. Hansen, C. A. Taatjes, J. Wang, T. A. Cool, S. Gon, P. R. Westmoreland, *Proc. Combust. Inst.* 31 (2007) 1119-1127.

25. M. Kamphus, M. Braun-Unkhoff, K. Kohse-Höinghaus, *Formation of small PAH in laminar premixed low-pressure propene and cyclopentene flames – experiment and modelling*, *Combust. Flame*, revised manuscript, July 2007.

26. T. Kasper, K. Kohse-Höinghaus, N. Hansen, C. A. Taatjes, M. E. Law, A. Morel, P. R. Westmoreland, J. Wang, T. A. Cool, *Species identification in laminar flames investigated by molecular beam mass spectrometry*, 5th US Combustion Meeting, San Diego, CA, USA, March 2007, paper no. A24.

27. C. A. Taatjes, N. Hansen, A. McIlroy, J. A. Miller, J. P. Senosiain, S. J. Klippenstein, F. Qi, L. Sheng, Y. Zhang, T. A. Cool, J. Wang, P. R. Westmoreland, M. E. Law, T. Kasper, K. Kohse-Höinghaus, *Science* 308 (2005) 1887-1889.

28. S. G. Lias, J. E. Bartmess, J. F. Liebman, J. L. Holmes, R. D. Levin, W. G. Mallard, *Ion energetics data, NIST Chemistry WebBook, NIST Standard Reference Database Number 69*, Eds. P. J. Linstrom, W. G. Mallard, S. A. Kafafi, June 2005, National Institute of Standards and Technology, Gaithersburg, MD, 20899, available at <http://webbook.nist.gov>.

29. A. Lamprecht, B. Atakan, K. Kohse-Höinghaus, *Combust. Flame* 122 (4) (2000) 483-491.

30. A. Lamprecht, B. Atakan, K. Kohse-Höinghaus, *Proc. Combust. Inst.* 28 (2000) 1817-1824.

31. G. González Alatorre, H. Böhm, B. Atakan, K. Kohse-Höinghaus, *Z. Phys. Chem.* 215 (2001) 981-995.

32. B. Atakan, A. Lamprecht, K. Kohse-Höinghaus, *Combust. Flame* 133 (2003) 431-440.

33. K. Kohse-Höinghaus, B. Atakan, A. Lamprecht, G. González Alatorre, M. Kamphus, T. Kasper, N.-N. Liu, *Phys. Chem. Chem. Phys.* 4 (2002) 2056-2062.

34. C. J. Pope, J. A. Miller, *Proc. Combust. Inst.* 28 (2000) 1519-1527.
35. H. Böhm, A. Lamprecht, B. Atakan, K. Kohse-Höinghaus, *Phys. Chem. Chem. Phys.* 2 (2000) 4956-4961.
36. K. Hoyermann, F. Mauß, T. Zeuch, *Phys. Chem. Chem. Phys.* 6 (14) (2004) 3824-3835.
37. R. P. Lindstedt, K.-A. Rizos, *Proc. Combust. Inst.* 29 (2002) 2291-2298.
38. N. Hansen, T. Kasper, S. J. Klippenstein, P. R. Westmoreland, M. E. Law, C. A. Taatjes, K. Kohse-Höinghaus, J. Wang, T. A. Cool, *J. Phys. Chem. A* 111 (19) (2007) 4081-4092.
39. T. S. Kasper, P. Oßwald, M. Kamphus, K. Kohse-Höinghaus, *Combust. Flame* 150 (3) (2007) 220-231.
40. N. Hansen, T. Kasper, P. Oßwald, T. A. Cool, K. Kohse-Höinghaus, unpublished results, 2006.
41. T. A. Cool, J. Wang, N. Hansen, P. R. Westmoreland, F. L. Dryer, Z. Zhao, A. Kazakov, T. Kasper, K. Kohse-Höinghaus, *Proc. Combust. Inst.* 31 (2007) 285-293.
42. P. Oßwald, U. Struckmeier, T. Kasper, K. Kohse-Höinghaus, N. Hansen, C. A. Taatjes, J. Wang, T. A. Cool, S. Gon, P. R. Westmoreland, *Experimental study of premixed propene/ethanol fuel blends, WIP Poster, 31st Int. Symp. on Combustion*, August 6-11, 2006, University of Heidelberg, Germany.
43. T. A. Cool, K. Nakajima, T. A. Mostefaoui, F. Qi, A. McIlroy, P. R. Westmoreland; M. E. Law, L. Poisson, D. S. Peterka, M. Ahmed, *J. Chem. Phys.* 119 (2003) 8356.
44. T. A. Cool, A. McIlroy, F. Qi, P. R. Westmoreland, L. Poisson, D. S. Peterka, M. Ahmed, *Rev. Sci. Instrum.* 76 (2005) Art. No. 094102.
45. C. A. Taatjes, N. Hansen, D. L. Osborn, K. Kohse-Höinghaus, T. A. Cool, P. R. Westmoreland, “*Imaging*” combustion chemistry via multiplexed synchrotron photoionization mass spectrometry, *Phys. Chem. Chem. Phys.* Invited feature article, submitted (2007).
46. N. Hansen, J. A. Miller, C. A. Taatjes, J. Wang, T. A. Cool, M. E. Law, P. R. Westmoreland, *Proc. Combust. Inst.* 31 (2007) 1157-1164.
47. a) Tina Kasper, *Molekularstrahlmassenspektrometrie zur Analytik in Flammen oxygenerter Brennstoffe*, PhD thesis, Cuvillier-Verlag, Bielefeld, 2007, ISBN-10: 3867273073, ISBN-13: 9783867273077, and b) T. Kasper, P. Oßwald, K. Kohse-Höinghaus, C.A. Taatjes, J. Wang, T. A. Cool, M. E. Law, A. Morel, P. R. Westmore-

land, *Isomeric propanol flames investigated by mass spectrometry, WIP Poster, 31st Int. Symp. on Combustion*, August 6-11, 2006, University of Heidelberg, Germany.

48. B. Yang, P. Oßwald, Y. Li, J. Wang, L. Wei, Z. Tian, F. Qi, K. Kohse-Höinghaus, *Combust. Flame* 148 (4) (2007) 198-209.

49. C. S. McEnally, L. D. Pfefferle, *Proc. Combust. Inst.* 30 (2005) 1363-1370.

50. P. Oßwald, U. Struckmeier, T. Kasper, K. Kohse-Höinghaus, J. Wang, T. A. Cool, N. Hansen, P. R. Westmoreland, *J. Phys. Chem. A* 111 (19) (2007) 4093-4101.

51. W. R. Schwartz, C. S. McEnally, L. D. Pfefferle, *J. Phys. Chem. A* 110 (2006) 6643-6648.

Figure Captions:

Figure 1: Quantitative species profiles in a C/O=0.5 propene-oxygen-argon (25%) flame at 40 mbar; measurements were obtained under nominally identical conditions during two different measurement cycles with VUV-PI-MBMS. Top left: propargyl radical, top right: benzene, bottom: acetylene.

Figure 2: Comparison of energy and mass resolution in a fuel-rich ethanol-oxygen-argon (25%) flame at 50 mbar. Top: EI-MBMS, bottom: VUV-PI-MBMS; the two-dimensional images show the measured signal for $m/z=44$ as a function of height above the burner (HAB), the diagrams on the right provide mass-resolved spectra at different HAB. *Adapted from [26].*

Figure 3: Fragmentation issues in EI-MBMS. *Adapted from [26].*

Figure 4: Selected species profiles in a fuel-rich ethanol flame measured by EI-MBMS (symbols) and VUV-PI-MBMS (lines). *Adapted from [26].*

Figure 5: Maximum signal intensities of aromatic molecules in ethanol-blended propene flames (C/O=0.6) with varying ethanol fraction in the fuel mixture. Signals are normalized to those in the unblended propene flame. Benzene: $m/z = 78$, toluene: $m/z = 92$, phenol: $m/z = 94$, indene: $m/z = 116$, naphthalene: $m/z = 128$. *From [39] with permission.*

Figure 6: Trends in the maximum mole fraction for different hydrocarbon species in ethanol-blended propene flames (C/O=0.5) with varying ethanol fraction in the fuel mixture. Ratios γ are defined as maximum mole fraction in the blended flame normalized by that in the pure propene flame.

Figure 7: Trends in the maximum mole fraction for key oxygenated species in ethanol-blended propene flames (C/O=0.5) with varying ethanol fraction in the fuel mixture. Ratios γ are defined as maximum mole fraction in the blended flame normalized by that in the pure ethanol flame.

Figure 8: Isomers of $m/z = 72$, identified in flames of the four isomers of butanol by their ionization energies. *From [48] with permission.*

Figure 9: Isomers of $m/z = 78$, identified in flames of the four isomers of butanol by their ionization energies. *From [48] with permission.*

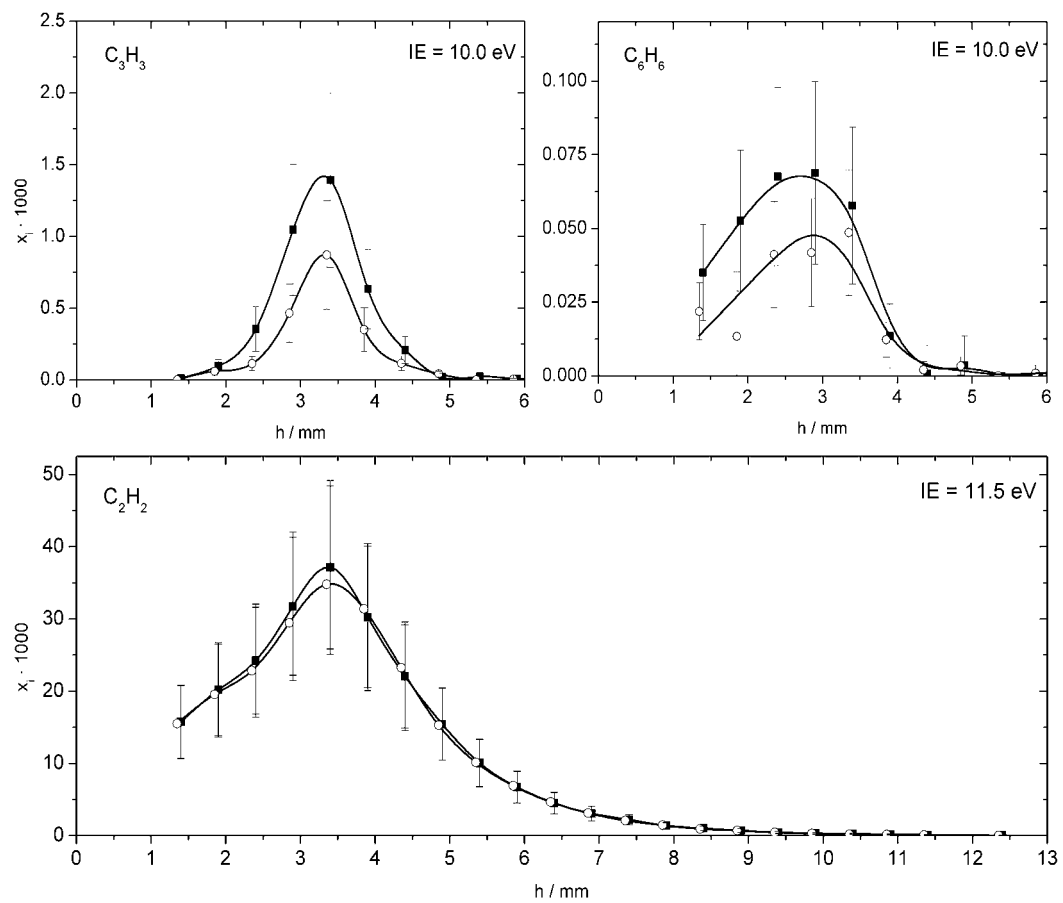
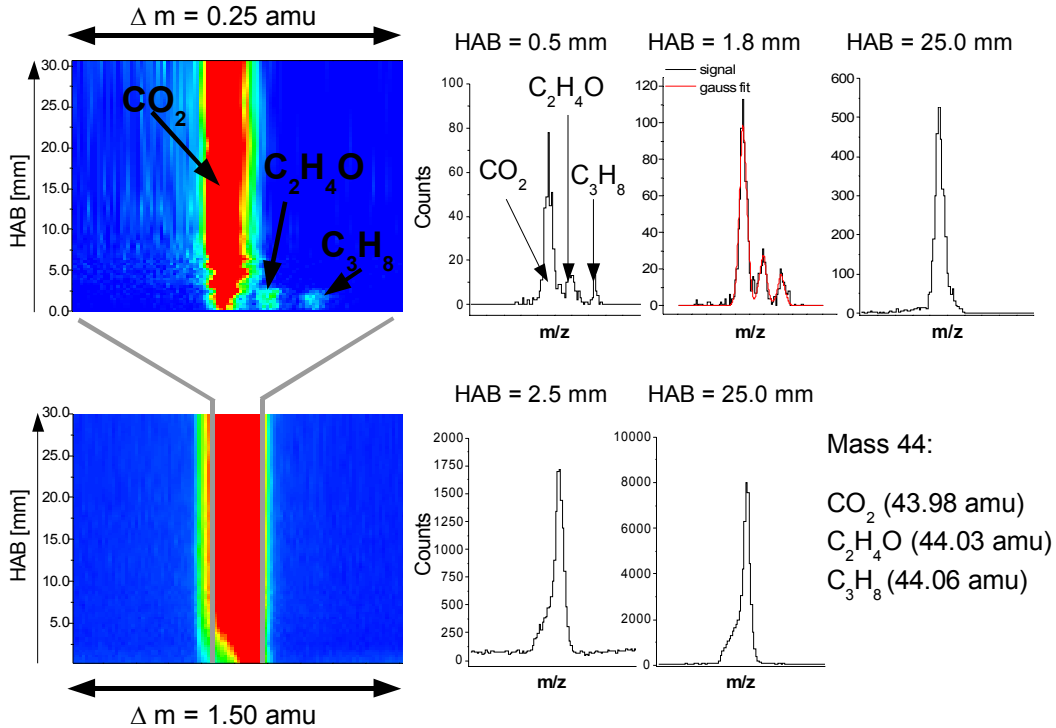


Figure 1: Quantitative species profiles in a C/O=0.5 propene-oxygen-argon (25%) flame at 40 mbar; measurements were obtained under nominally identical conditions during two different measurement cycles with VUV-PI-MBMS. Top left: propargyl radical, top right: benzene, bottom: benzene.

EI, TOF: $m/\Delta m=3000$



PI, TOF: $m/\Delta m=400$

Figure 2: Comparison of energy and mass resolution in a fuel-rich ethanol-oxygen-argon (25%) flame at 50 mbar. Top: EI-MBMS, bottom: VUV-PI-MBMS; the two-dimensional images show the measured signal for $m/z=44$ as a function of height above the burner (HAB), the diagrams on the right provide mass-resolved spectra at different HAB. *Adapted from [26].*

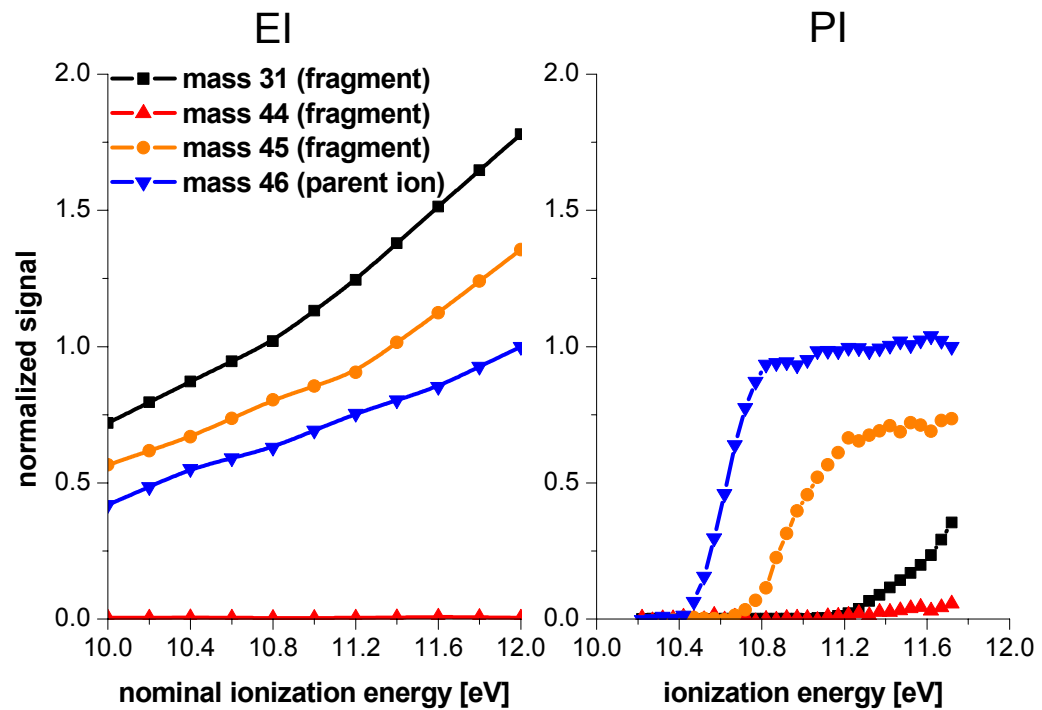


Figure 3: Fragmentation issues in EI-MBMS. *Adapted from [26].*

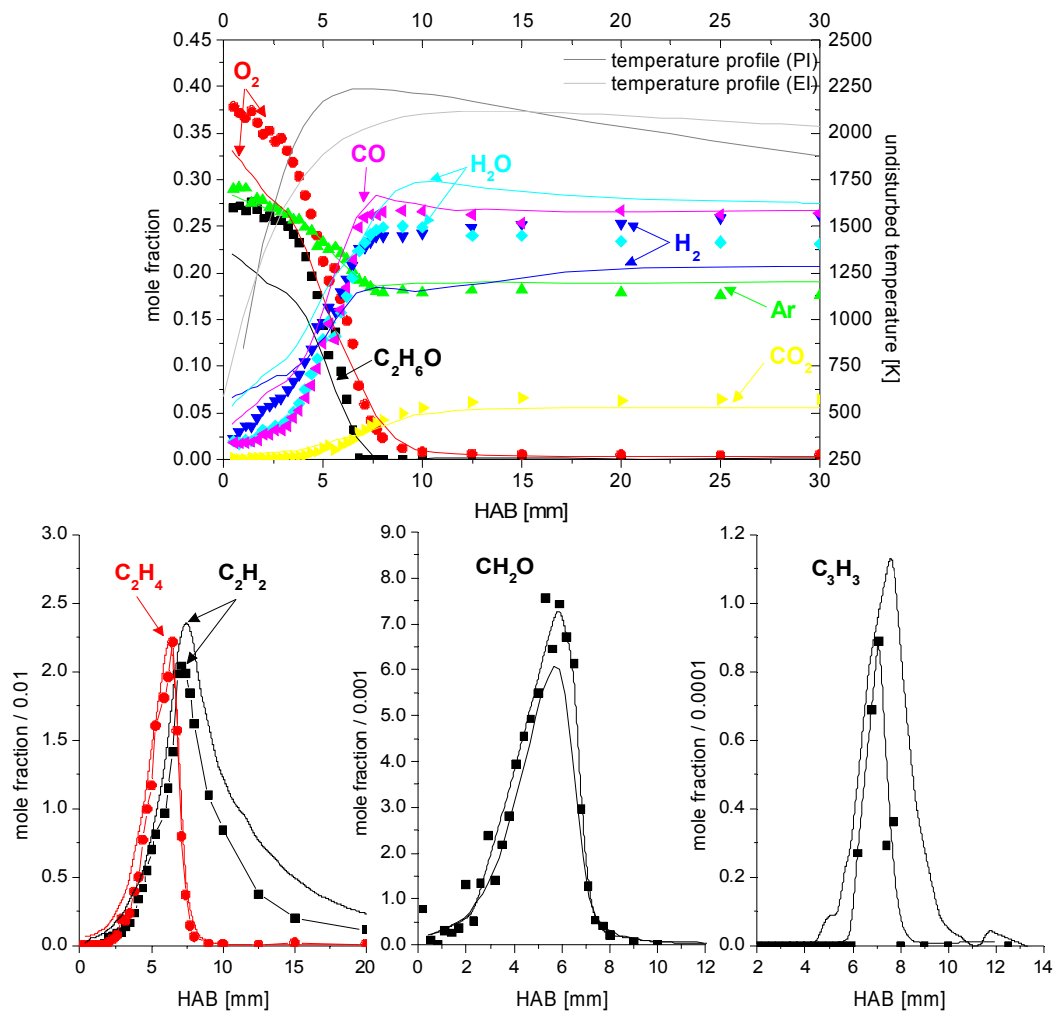


Figure 4: Selected species profiles in a fuel-rich ethanol flame measured by EI-MBMS (symbols) and VUV-PI-MBMS (lines). *Adapted from [26].*

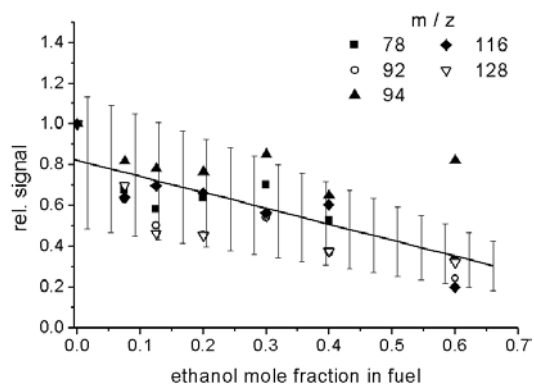


Figure 5: Maximum signal intensities of aromatic molecules in ethanol-blended propene flames (C/O=0.6) with varying ethanol fraction in the fuel mixture. Signals are normalized to those in the unblended propene flame. Benzene: $m/z = 78$, toluene: $m/z = 92$, phenol: $m/z = 94$, indene: $m/z = 116$, naphthalene: $m/z = 128$. *From [39] with permission.*

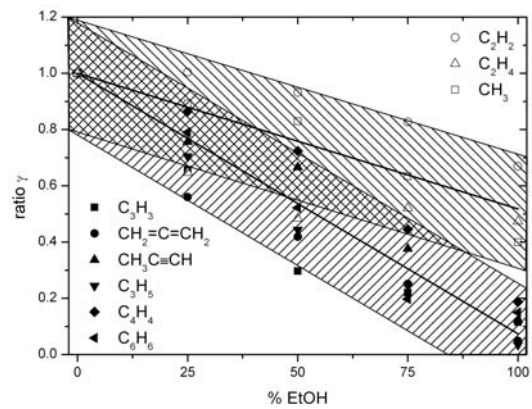


Figure 6: Trends in the maximum mole fraction for different hydrocarbon species in ethanol-blended propene flames ($\text{C}/\text{O}=0.5$) with varying ethanol fraction in the fuel mixture. Ratios γ are defined as maximum mole fraction in the blended flame normalized by that in the pure propene flame.

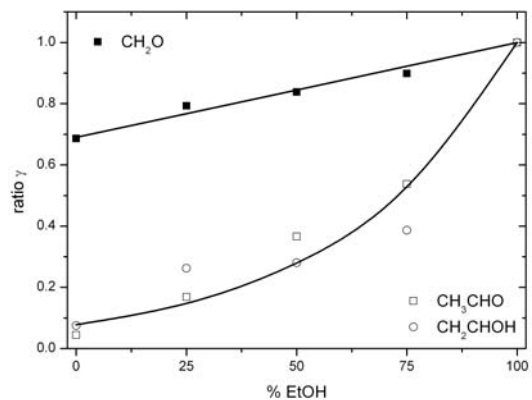


Figure 7: Trends in the maximum mole fraction for key oxygenated species in ethanol-blended propene flames (C/O=0.5) with varying ethanol fraction in the fuel mixture. Ratios γ are defined as maximum mole fraction in the blended flame normalized by that in the pure ethanol flame.

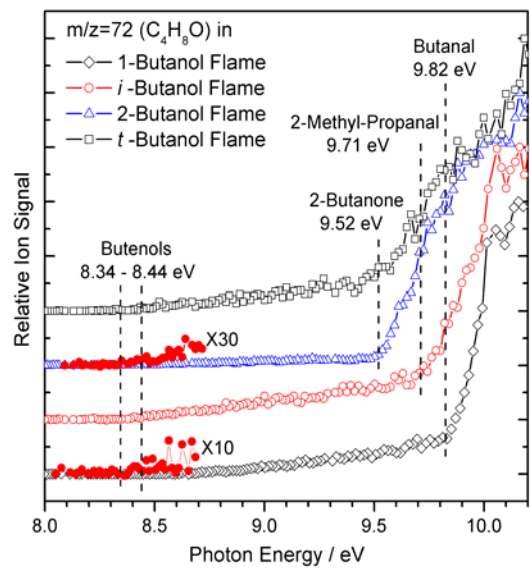


Figure 8: Isomers of $m/z = 72$, identified in flames of the four isomers of butanol by their ionization energies. *From [48] with permission.*

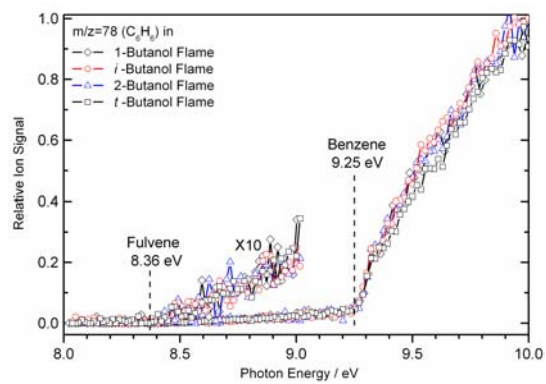


Figure 9: Isomers of $m/z = 78$, identified in flames of the four isomers of butanol by their ionization energies. *From [48] with permission.*